Designing Highly Luminescent Molecular Aggregates via Bottom-Up Nanoscale Engineering

Ulugbek Barotov,[†] Megan D. Klein,[†] Lili Wang[†] and Moungi G. Bawendi[†]*

Department of Chemistry, Massachusetts Institute of Technology, 77 Massachusetts Avenue, Cambridge, Massachusetts 02139, United States

ABSTRACT

Coupling of excitations between organic fluorophores in J-aggregates leads to coherent delocalization of excitons across multiple molecules, resulting in materials with high extinction coefficients, long-range exciton transport, and, in particular, short radiative lifetimes. Despite these favorable optical properties, uses of J-aggregates as high-speed light sources have been hindered by their low photoluminescence quantum yields. Here, we take a bottom-up approach to design a novel J-aggregate system with a large extinction coefficient, a high quantum yield and a short lifetime. To achieve this goal, we first select a J-aggregating cyanine chromophore and reduce its nonradiative pathways by rigidifying the backbone of the cyanine dye. The resulting conformationally-restrained cyanine dye exhibits strong absorbance at 530 nm and fluorescence at 550 nm with 90% quantum yield and 2.3 ns lifetime. We develop optimal conditions for the self-assembly of highly emissive J-aggregates. Cryogenic transmission electron microscopy (cryo-TEM) and dynamic light scattering (DLS) reveal micron-scale extended structures with 2D sheet-like morphology, indicating long-range structural order. These novel J-aggregates have a strong red-shifted absorption at 600 nm, resonant fluorescence

with no Stokes shift, 50% quantum yield, and 220 ps lifetime at room temperature. We further stabilize these aggregates in a glassy sugar matrix and study their excitonic behavior using temperature-dependent absorption and fluorescence spectroscopy. These temperature-dependent studies confirm J-type excitonic coupling and superradiance. Our results have implications for the development of a new generation of organic fluorophores that combine high speed, high quantum yield and solution processing.

KEYWORDS: J-aggregate, superradiance, conformational restraint, high-speed materials, cyanine dyes, photoluminescence, quantum yield

INTRODUCTION

Decades of research on the fundamental properties of exciton behavior in organic molecules and semiconductor quantum dots have resulted in fluorescent materials with strong absorption cross sections, tunable Stokes' shifts, and near unity quantum yields, spanning a wide range of the electromagnetic spectrum.[1,2] There have been significant developments in understanding materials that exhibit aggregation-induced emission, resulting in tunable, robust, and highly efficient fluorescence in the solid-state.[3,4] These advanced fluorophores have been used in a wide range of applications, including in displays, lasing, and deep-tissue biomedical imaging.[1,2,5] Despite their favorable optical properties, application of these materials as high-speed light sources have been hindered by their intrinsically long lifetimes, typically above 1 ns.[6] Many applications, including high-speed free space optical communication, lifetime-resolved biomedical imaging and quantum communication, require materials that exhibit strong absorption cross sections, high quantum yields, and short radiative lifetimes (<1 ns).

The radiative rate of organic molecules, quantum dots, and semiconductor quantum wells can be enhanced by changing their local fields using plasmonic nanostructures.[7–9] However, a concomitant increase in non-radiative losses limits their overall quantum efficiency.[10] In addition, directional emission and a strong dependence of the enhancement on emitter-nanoparticle separation complicate integration of such materials into waveguides and devices. An alternative avenue for high-speed fluorescent materials is through the superradiance phenomenon, which is observed in diatomic arrays,[11] quantum dots assemblies[12] and molecular J-aggregates.[13] Coherent coupling of excitations leads to the delocalization of excitons over several emitters and collective fluorescence. For J-aggregates, enhancement factors or coherence lengths of up to 200 monomers have been observed at low temperatures.[14,15] As the temperature increases, the coherence length decreases due to increased homogeneous disorder. Nevertheless, J-aggregates are still one of the fastest fluorophores known, with observed lifetimes as low as 100 ps at room temperature in solution. In addition to fast radiative rates, J-aggregates have strong absorption, narrow photoluminescence linewidth, and efficient long-range exciton transport. Recently, micron length exciton transport was reported for the double-walled nanotubular J-aggregates of C8S3 through exciton-exciton annihilation experiments.[16] Strong absorption, narrow photoluminescence, and short lifetimes make J-aggregates excellent fluorophores for fast optoelectronic applications.

Despite the favorable properties of J-aggregates, their use as high-speed light sources has been limited due to their low photoluminescence quantum yields (QYs) at room temperature. For instance, J-Aggregates of C8S3 have only a 15% QY,[17] J-Aggregates of TDBC have a 26% QY,[18] and the first discovered and most widely studied J-aggregates of pseudoisocyanine chloride have a 28% QY at room temperature.[19] Many J-Aggregates emitting in the visible and NIR have QYs below 10%.[20–22] The low QY of J-Aggregates has been attributed to large homogenous and inhomogenous disorder,[14,23] charge-transfer states,[14]

vibronic coupling and self-trapped excitons.[24–26] The type of nonradiative pathways dominant in a J-aggregate is different for different classes of chromophores. In order to develop J-aggregates with high QYs, nanoscale engineering strategies should be tailored for a given class of J-aggregates. For instance, disorder and charge-transfer states dominate nonradiative processes in J-aggregates of some perylene bisimide chromophores. It was shown that reducing disorder and suppressing the formation of charge-transfer states lead to 100% QY in high quality 2D monolayers of J-aggregates.[14] However, high temperature fabrication protocols used in this work is not suitable for most J-aggregates, including widely studied J-aggregates of cyanine dyes. Another strategy to improve the fluorescence quantum efficiency of J-aggregates is to influence their molecular packing and morphology using small molecules and surfactants.[18,20,27] Recently, Anantharaman et al. reported the use of alkylamines, specifically ethylamine and hexylamine, to increase the QY of TDBC J-aggregates to 60%.[27] Hexylamine and water form bicontinuous phase microemulsion, where J-aggregates are stabilized at the interphase of nanoscale-sized water and hexylamine domains, restricting the size of J-aggregates and reducing exciton quenching at lattice defects. More precise control of molecular packing, morphology, and solvent nanostructure at the nanoscale is needed to extend this approach to other J-aggregate systems.

Cyanine dyes represent a major class of tunable chromophores which cover the visible, NIR and short-wave infrared (SWIR) regions of the electromagnetic spectrum.[28,29] The fluorescence quantum efficiency of most cyanine dyes suffers from excited-state C-C rotational deactivations, which occur at picosecond timescales.[30,31] Even though the coupling of excitations to vibrational motions is significantly reduced as molecules pack into J-aggregate lattices, static and dynamic disorder limit the magnitude of this effect, leading to low QYs in J-aggregates. In this work, we take a bottom-up approach to develop highly emissive J-aggregates. We first reduce nonradiative pathways in a J-aggregating cyanine dye by

rigidifying its backbone using a six-membered fused ring system. Next, we develop optimal conditions that lead to the self-assembly of highly emissive J-aggregates. Rigidifying the backbone of cyanine dyes through conformational restraint around the polymethine backbone is well-established in the context of fluorescent tags for biological imaging.[32,33,28] However, such dyes have traditionally been functionalized with bulky groups, which prevents the formation of any kind of aggregate. Cyanine conformational restraint applied to the development of highly emissive J-aggregates has not been explored. In addition, J-aggregates were historically used for their strong absorption and transport properties in silver halide photography.[34–36] In their application in photography, it was beneficial to have J-aggregates with low quantum yields since photon emission would reduce photographic contrast. There has been an exploration of rigidified dyes as spectral sensitizers, but, to our knowledge, not to the development of highly emissive J-aggregates.[37]

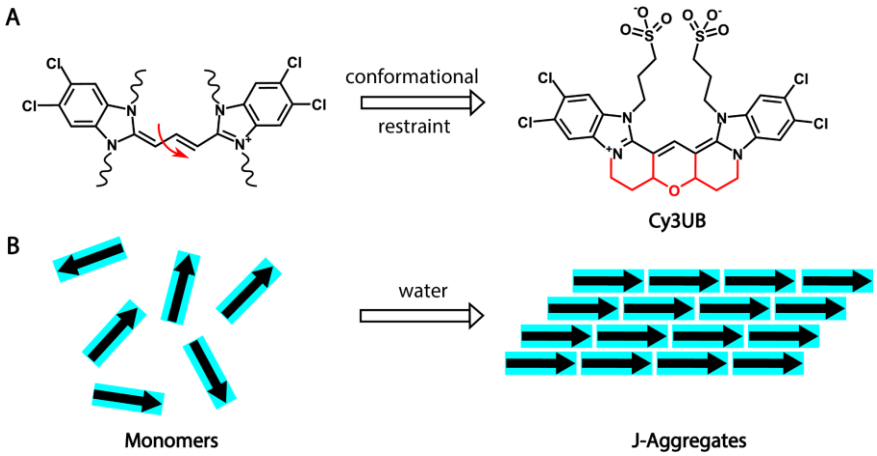

Figure 1. Overview of the study. (**A**) We investigate the optical properties of J-aggregates of a novel cyanine dye with a rigidified backbone (right). This is in contrast to most widely studied J-aggregating dyes with flexible backbones (left). (**B**) After the synthesis of the dye, we explore conditions which lead to J-aggregates with excellent fluorescence properties. Black arrows represent transition dipole moments of molecules.

We designed and synthesized a novel cyanine dye with a chromophore that was expected to form J-aggregates (Fig. 1A, right). The dye includes a six-membered fused rings system around its trimethine backbone to reduce nonradiative relaxation pathways and increase its QY. We chose a small, charged alkylsulfonate side group to allow aggregation of the dye in water-methanol mixtures. After the synthesis of the dye, we studied its aggregation behavior (**Fig. 1B**). We find that the rigidified dye Cy3UB has 90% QY in methanol with a lifetime of τ = 2.3 ns. When water is added to the methanol solution of the dye, an equilibrium is established between the solvated monomers and the J-aggregates. Using cryogenic transmission electron microscopy (cryo-TEM) and dynamic light scattering (DLS) experiments, we characterized the size and morphology of the aggregates. We observed micron-scale extended structures with a 2D sheet-like morphology, indicating long-range structural order. We find that J-aggregates of Cy3UB have a strong absorption at 600 nm, resonant fluorescence with no Stokes shift, 50% quantum yield, and 220 ps lifetime at room temperature. We further stabilized J-aggregates in a glassy sugar matrix and studied their excitonic behavior using temperature-dependent absorption and emission spectroscopy. The temperature-dependent studies confirm J-type excitonic coupling between constituent molecules, which is necessary to obtain strongly fluorescent materials in condensed phases. Our results have major implications for the development of highly emissive J-aggregates using bottom-up nanoscale engineering.

METHODS

Synthesis of Cy3UB. Detailed description of the synthetic protocols and thorough characterization of the intermediates is provided in the **SI**.

Preparation of Cy3UB J-Aggregates. The alcoholic route was used for the assembly of the novel Cy3UB J-Aggregates. Briefly, highly purified Cy3UB dye was added to methanol

(>99.9%, VWR, EM-MX0488-1), sonicated, and gently heated to prepare 5.2 mM stock solution. Under a nitrogen atmosphere inside a glove bag, 40 µL of the Cy3UB stock solution was added to a vial that was pre-soaked in water overnight. Subsequently, 400 µL of ultrapure water (Miili-Q, 18 MΩ·cm, Thermo Fisher Scientific) was added to the vial and gently shaken to ensure a homogenous solution. An immediate color change from orange to purple was observed, indicating the formation of J-aggregates. The sample was wrapped with aluminum foil and stored in the dark for 4-7 days to yield highly emissive J-aggregates.

Cryo-TEM. To prepare J-aggregate samples for cryo-imaging, 200 mesh copper grids with quantifoil holey carbon support films (Quantifoil R, 3.5/1, EMSDIASUM, Q225CR-35) were hydrophilized by glow discharging in an EMITech K100X for 60 seconds at 20 mA. 3 µL of the J-aggregate solution was applied onto grids. Excess solution was removed from the grids by blotting the sample using Vitrobot Mark IV (Thermo Fisher Scientific). The sample was then immediately plunged into liquid ethane to flash freeze and stabilize the J-aggregates in aqueous solution at approximately -175^{0}C. The grids were transferred under liquid nitrogen (LN2) into the LN2-cooled autoloader and the sample stage of a Talos Arctica G2 cryoTEM (Thermo Fisher Scientific) for imaging under minimal dose, which was essential to prevent J-aggregate degradation under the electron beam. The microscope was operated at 200 kV and a magnification in the range of 10,000X – 60,000X. To enhance contrast, images were collected with -10 µm underfocus. All images were recorded using a Falcon 3EC direct electron detector (Thermo Fisher Scientific) operated in linear mode.

Quantum Yield Measurement. Quantum yields of Cy3UB monomer and the J-aggregate were obtained using the relative method as previously described.[38,39] Rhodamine 6G with 93% QY in methanol was used as a standard. Briefly, a series of different concentrations of rhodamine 6G was prepared by dissolving the dye in methanol and diluting it to an appropriate extent. Different concentrations of J-aggregates were prepared by gently diluting

the J-aggregate stock solution with water and allowing them to equilibrate for 30 mins. To obtain the QY of Cy3UB monomer in methanol, all measurements were taken using 1 cm quartz cuvettes. To obtain the QY of Cy3UB J-aggregates, all measurements for rhodamine 6G and J-aggregate solutions were collected using 0.1 mm and 0.01 mm quartz cuvettes (Starna), respectively. Fluorescence spectra were collected by exciting rhodamine 6G, Cy3UB monomer, and J-aggregate samples at 500 nm, 500 nm, and 570 nm, respectively. Absorption spectra, emission spectra, and calibration plots for the quantum yield measurements are provided in the **SI**.

Absorption and Emission Spectroscopy. Absorption spectra were collected on a Cary 5000 Spectrometer (Agilent). Fluorescence spectra were collected on a FluoroMax fluorometer (Horiba Scientific). In order to carry out temperature-dependent absorption and emission studies, J-aggregates were first stabilized in a glassy sugar matrix following a previously described method.[16,17] 3 mL milli-Q water was added to the mixture of 2 g sucrose (Sigma) and 2 g trehalose (Sigma), and mixed vigorously to obtain a saturated sugar solution. 100 µL the sugar solution was slowly added to 100 µL of the J-Aggregate stock solution, and mixed gently to obtain a homogenous solution. 50 µL of the resulting J-aggregate sugar solution was deposited onto a 0.1 mm demountable quartz cuvette and dried under 0.5 atm vacuum for a day. To carry out temperature-dependent studies, dried J-aggregate sugar samples were put in a cold finger cryostat (Janis Research Co., ST-100) and evacuated using a Varian pump (Varian 9698222) for 4 hours. The sample was cooled down under a constant flow of liquid nitrogen. The temperature was adjusted using a LakeShore 330 Autotuning temperature controller. All of the temperature-dependent absorption measurements were performed on a Cary 5000 Spectrophotometer (Agilent) and all of the temperature-dependent fluorescence measurements were collected on a home-built PL setup.

Time-Resolved Photoluminescence Spectroscopy. Samples were excited with the 404 nm doubled output of a Ti:Sapph oscillator (78 MHz, Coherent Mira 900-F) focused through a lens (f = 20 cm). Excitation powers were measured on a photodiode power meter (Thorlabs S121C). Emission was collected with a pair of 2 in. parabolic mirrors and focused into a spectrometer (Bruker 250IS) with a 300 groove/mm grating. The spectrally dispersed output from the spectrometer was then directed into a streak camera (Hamamatsu C5680) with an attached syncroscan sweep unit (Hamamatsu M5675). Streak images were collected with 100 ms integration time and 100 integrations. Image analysis and emission decay trace fitting were performed using a homebuilt Matlab library.

RESULTS AND DISCUSSION

Synthesis and Characterization of the Rigidified Dye Cy3UB. The structure of the dye studied in this paper is given in **Fig. 1A** (right). Inspired by the naming convention of the analogous rigidified cyanine dyes, we named this novel molecule Cy3UB. A synthetic route (**Scheme 1**) was developed based on the available literature on similar reactions.[33,40,41,42]

Scheme 1. Four-step synthetic route to Cy3UB

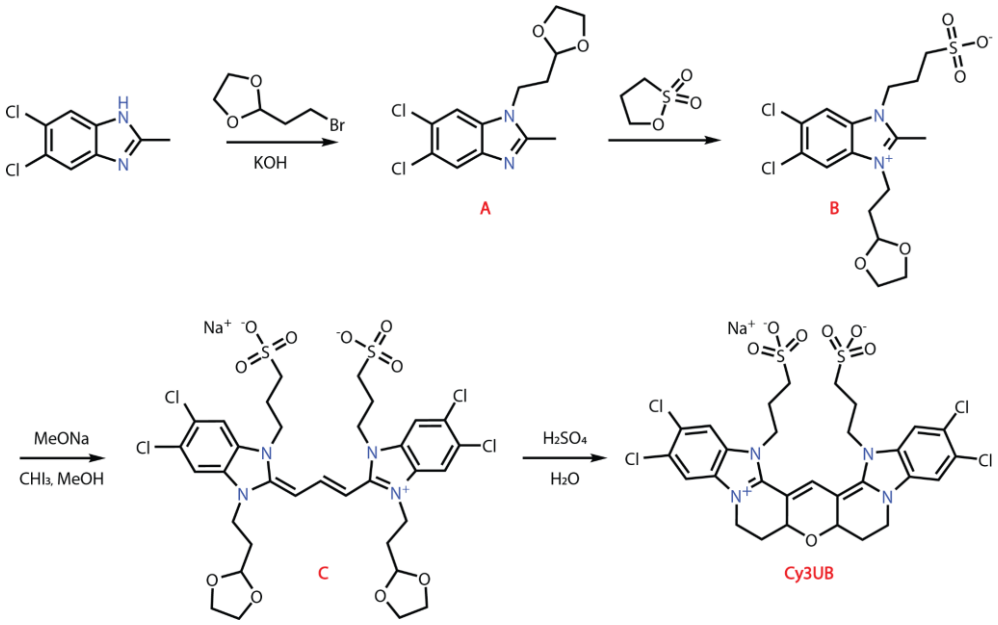

Briefly, 5,6-dichloro-2-methyl-benzimidazole was treated with bromoethyl-1,3-dioxolane in the presence of KOH to yield 1-(2-(1,3-dioxolan-2-yl)ethyl)-5,6-dichloro-1-methyl-benzimidazole (Compound **A**). In the next step, compound **A** was reacted with propane sultone to afford sulfopropyl-substituted intermediate compound **B**. Condensation of two equivalents of compound **B** with iodoform resulted in the highly colored dye **C**. In the final step, compound **C** was treated with sulfuric acid to hydrolyze the acetal groups and form six-membered rings around the polymethine backbone to yield the Cy3UB dye. Due to concerns with photooxidative damage to dyes, compound **C** and Cy3UB were handled carefully to minimize exposure to light (see Supporting Information). ^{1}H NMR of Cy3UB in deuterated methanol (Fig. 2A) confirms the proposed structure. Detailed description of the synthetic protocols and thorough characterization of the intermediates is given in the **SI**.

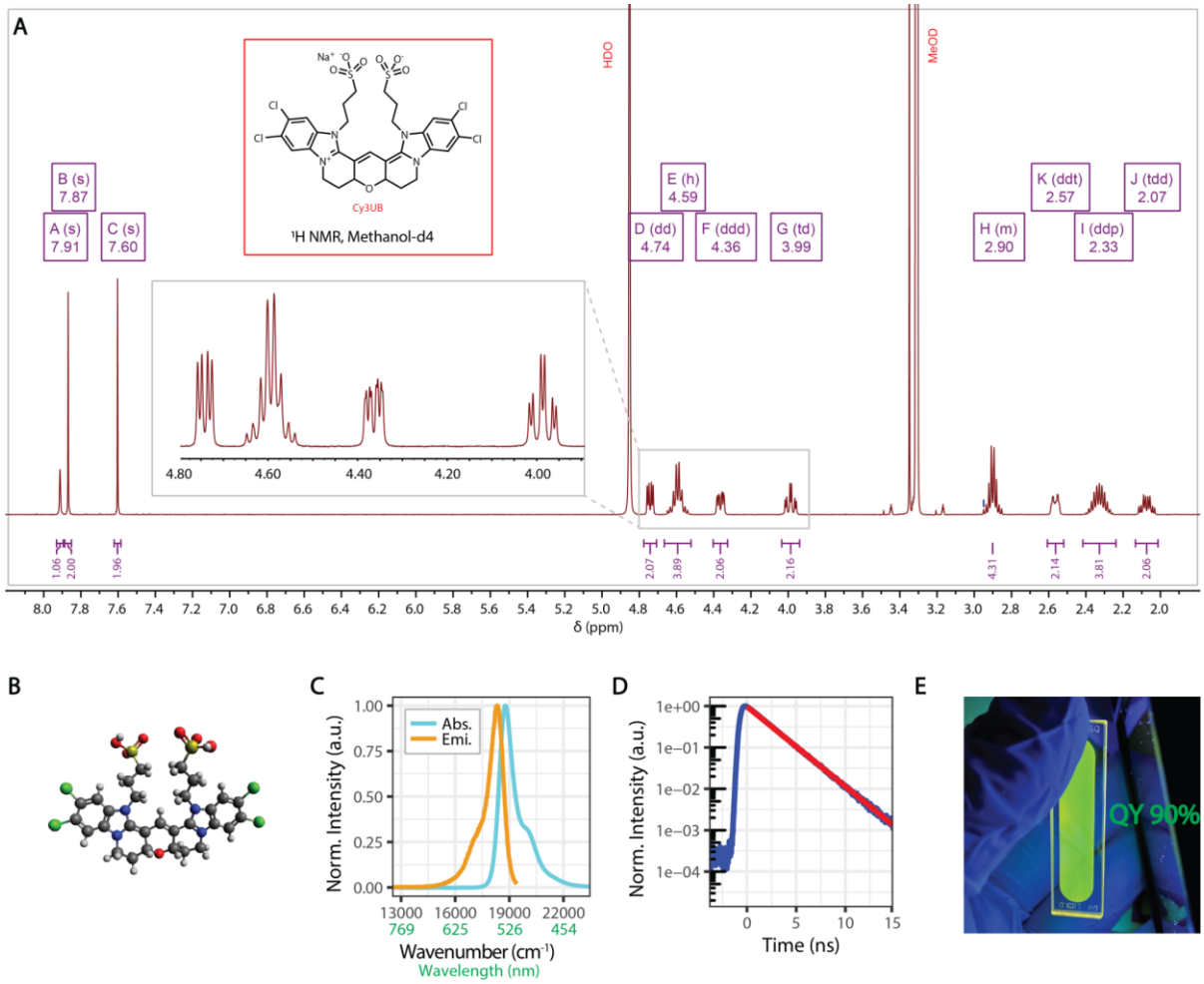

Figure 2. Characterization of the cyanine dye Cy3UB. (**A**) ^{1}H NMR spectroscopy confirms the structure of Cy3UB. (**B**) DFT calculations indicate that the geometry of the chromophore is planar with a small angle between the two heterocyclic aromatic groups. (**C**) Absorption and emission spectra of the dye solvated in methanol. (**D**) Time-resolved photoluminescence spectrum (blue curve) with a monoexponential fit (red line, τ = 2.3 ns). (**E**) PL image of the dye solvated in methanol under UV irradiation. The quantum yield in methanol is 90%.

Geometry of Cy3UB was optimized at the RHF/def-SVP level of theory[43] using the ORCA program (version 4.2.1). DFT calculations indicate that the geometry of Cy3UB is essentially planar with a small angle between the two heterocyclic aromatic groups (Fig. 2B). Absorption and emission spectra of the dye dissolved methanol is given in Fig. 2C. Incorporation of six-membered rings around the polymethine backbone reduces the vibrational degrees of freedom in the molecule, leading to narrow absorption and emission envelopes. Additionally, rigidification of the dye leads to an improved quantum efficiency and extended lifetime. We find that the rigidified dye has 90% QY in methanol, which is in stark contrast to the low QYs observed in open-chain analogues such as the 3% QY in TDBC (see SI). The time-resolved PL decay of Cy3UB was fitted using a monoexponential with a 2.3 ns lifetime (Fig. 2D), which is an order of magnitude longer than the observed lifetimes of low QY unrigidized open-chain counterparts. The PL image of the dye under UV excitation is shown in Fig. 2E. These findings are consistent with the fact that nonradiative relaxation pathways in cyanine dyes are associated with C-C rotations within the polymethine backbone. Recently, a previously unobserved optically-dark charge-transfer state was observed along the photoisomerization pathway of Cy3 molecule using transient gratings spectroscopy.[31] Formation of the dark state occurs within 1 ps of photoexcitation through coupling to vibrational modes, which persist for 1.5 ps after photoexcitation. Rigidification of the polymethine backbone through conformational restraint leads to significantly reduced C-C

rotational deactivations, making the radiative process the dominant relaxation pathways for excitons.

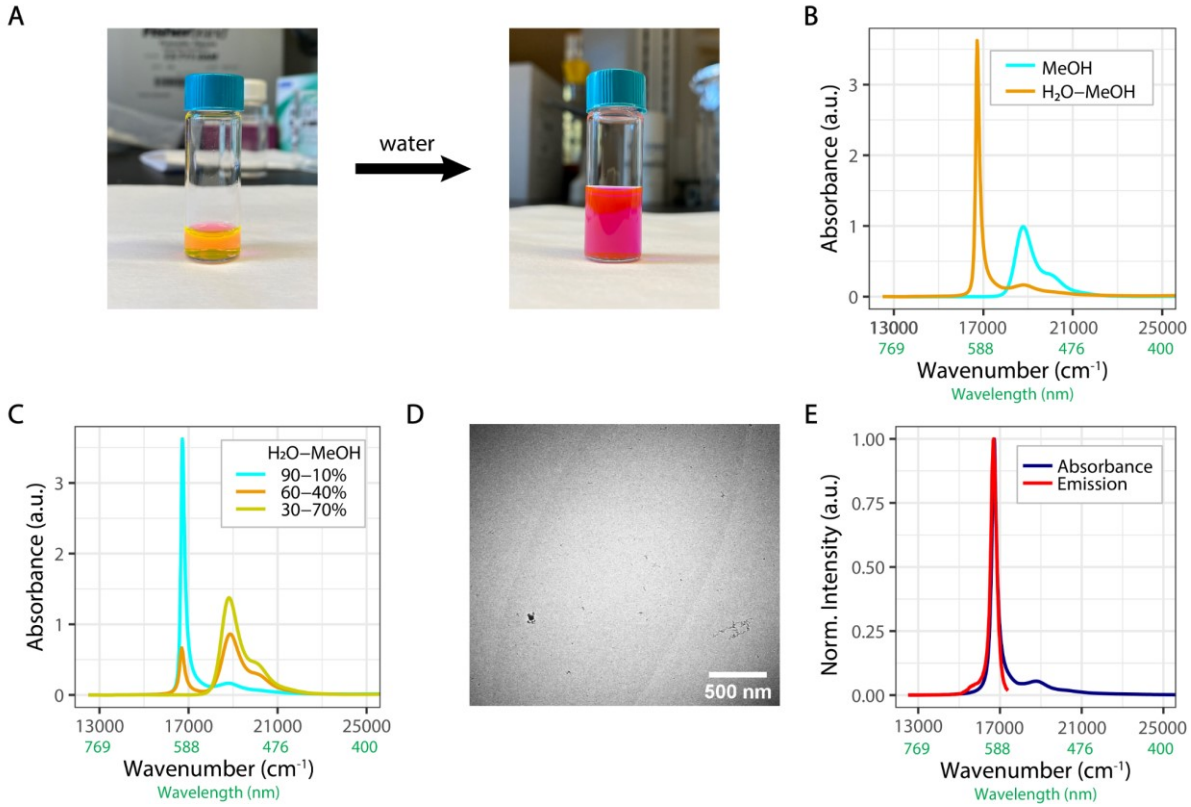

Figure 3. Characterization of J-aggregates of Cy3UB. (**A**) Addition of milli-Q water to the methanol solution of Cy3UB (left) leads to the formation of J-aggregates (right) accompanied by a strong color change. (**B**) Steady-state absorption spectroscopy reveals the formation of an intense, narrow, and red-shifted absorption peak, consistent with the formation of J-aggregates. (**C**) Solvent composition strongly dictates the fraction of J-aggregates formed. Here, we fix the concentration of the dye at 0.49 mM while varying the water-to-methanol ratio. Below 30% water fraction, only the monomer peak is observed. As the percentage of water is increased, the equilibrium shifts towards the J-aggregates. (**D**) A cryo-TEM micrograph reveals the micron-scale 2D sheet-like morphology of the J-aggregate. The scale bar is 500 nm. (**E**) The absorption and emission spectra of Cy3UB J-aggregates, showing a negligible Stoke's shift.

Characterization of J-aggregates of Cy3UB in Water-Methanol Mixtures. Motivated by the optical properties of the rigidized dye, we next investigated whether this dye

forms highly emissive J-aggregates with short lifetimes. Addition of water to the methanol solution of the dye (Fig. 3A, left) results in a strongly purple colored J-aggregate solution (Fig. 3A, right). Steady-state absorption spectroscopy reveals the formation of an intense, narrow and red-shifted absorption peak compared to the solvated monomer in methanol (Fig. 3B). The absorption peak redshifts from 18,797 cm^{-1} (532 nm) to 16,667 cm^{-1} (600 nm), whereas the full-width at half maximum (FWHM) of the absorption peak is reduced from 960 cm^{-1} (27 nm) to 280 cm^{-1} (10 nm). These spectral changes are characteristics of I- or J-aggregate formation, where a redshift and a reduced FWHM arise due to transition dipole moment coupling and motional narrowing, respectively.[22,23,44,45] In addition to a red-shifted I-state, I-aggregates have dark states below the bright state, leading to the quenching of the exciton fluorescence.[22,45] Therefore, it is necessary to favor J-type excitonic coupling to get fluorescent aggregates. In the next section, we perform temperature dependent absorption and emission spectroscopy to confirm J-type excitonic coupling in Cy3UB aggregates.

We explored the solvent-composition-dependent equilibrium between the Cy3UB monomers and the J-aggregates. The alcoholic route[46,47,48] used here for the self-assembly of J-aggregates allows convenient control of the water-to-methanol ratio, which was tuned from 0% to 100%. Selected absorption spectra for different solvent compositions are shown in Fig. 3C. Below a water concentration of 30%, only monomer peaks are observed. As the percentage of water is increased, a surge in J-aggregate intensity along with a concomitant decrease in monomer intensity is observed. Throughout the explored phase diagram, no H-aggregate feature, characterized by blue-shifted absorption peaks,[44,49,50] was detected. This is in contrast to the equilibrium of many other J-aggregating dyes such as pseudoisocyanine chloride in water,[35,51–53] where monomers, H-aggregates, and J-aggregates are all present simultaneously at high concentrations. We hypothesize that H-aggregates of Cy3UB are not observed due to hindered cofacial stacking resulting from the presence of four halogen atoms at the vertices of

Cy3UB. Cryogenic transmission electron microscopy (cryo-TEM) of vitrified samples in water reveal the two-dimensional sheet-like morphology of the aggregates with long-range structural order spanning several microns. The 1.9 μm average size obtained by sampling a larger number of aggregates using dynamic light scattering (DLS) measurements was consistent with the results of the cryo-TEM experiment. Thermodynamics of self-assembly and thorough morphological characterization of a few other molecular aggregates spanning visible and near-infrared were reported recently.[54]

Absorption and emission spectra of the Cy3UB J-aggregates are shown in Fig. 3E. The timescale at which excitons coherently delocalize along the aggregate is much faster compared to the timescale of nuclear rearrangements. Therefore, coupling of exciton states to the environment is significantly reduced in the aggregate compared to that in a solvated molecule. This leads to a resonant fluorescence and a negligible Stoke's shift in molecular J-aggregates.[25,55] Due to the latter property, highly concentrated solutions of J-aggregates suffer from detrimental self-reabsorption losses, which can be overcome using hybrid molecular aggregate architectures with the introduction of artificial Stoke's shift. The extent of exciton delocalization is limited by static and dynamic disorder. As a result, we observe a small vibronic progression in the emission spectrum. Using experimental data, we obtain an exciton delocalization length (N_c) ~ 17 monomers at room temperature. To quantify the efficiency of fluorescence, we used the relative method as previously described.[38,39] We prepared J-aggregate and Rhodamine 6G samples at different concentrations, and measured their absorbance and emission spectra. Calibration plots (Fig. 4A) were generated and used to calculate 50% QY for the J-aggregates. Since the monomer has a near unity quantum yield, we attribute competing nonradiative rates to imperfections specific to the J-aggregate lattice, such as trace impurity quenchers, charge transfer states, and faulty stacking. Fig. 4B shows the PL image of the J-aggregate under UV excitation. We observed a strong dependence of the PL QY

on the purity of the dye. In order to get highly emissive J-aggregates, it was essential to use extensively purified dye. This is consistent with the findings that extended structural order and strong excitonic coupling between molecules lead to long range exciton transport in J-aggregates.[15,16,56,57] Excitations formed in these systems can migrate long distances to find low energy traps or quenchers, resulting in a strong dependence of PL QY on any impurities in the system.

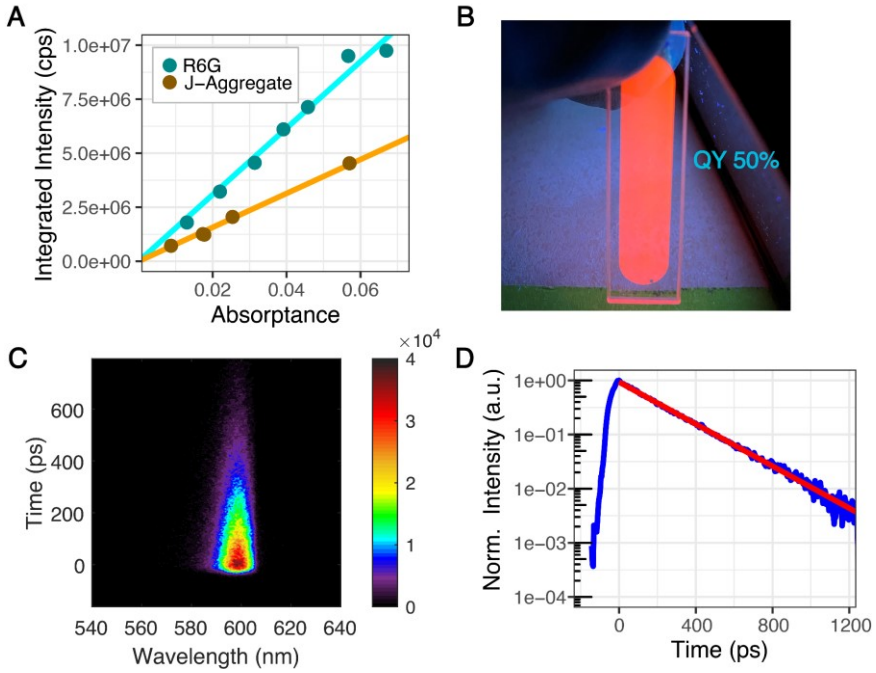

Figure 4. Strong Fluorescence from the Cy3UB J-Aggregates. (**A**) Plot of integrated emission as a function of absorptance for rhodamine 6G (cyan) and Cy3UB J-aggregates (orange). The QY of the Cy3UB J-aggregates was found to be 50%. (**B**) The PL image of the J-aggregates under UV light. (**C**) Streak camera image showing the time evolution of J-aggregate fluorescence. (**D**) Time-resolved photoluminescence of Cy3UB J-aggregates (blue) with a monoexponential fit (τ = 220 ps, red).

Coherent excitonic interactions give rise to increased radiative rates, leading to very short emission lifetimes.[13,14,34] To confirm the superradiance in J-aggregates of Cy3UB, we measured their lifetime using time-resolved photoluminescence (TRPL) spectroscopy. Figure 4C shows the time evolution of the J-aggregate photoluminescence. Figure 4D shows the

integrated TRPL decay curve, which was fit using a monoexponential function with a lifetime of τ = 220 ps. So, upon formation of J-aggregates, the radiative rate of excitons increased 5.7 fold from $4.0 \cdot 10^8\ \square^{-1}$ (in methanol) to $2.3 \cdot 10^9\ \square^{-1}$ (in water). For J-aggregates with such a short lifetime, a 50% QY in solution is among the highest reported in the literature. Comparison of the QY of the monomer in methanol (90%) and the J-aggregate (50%) highlights fundamental properties of exciton decay channels in J-aggregates. In addition to nonradiative pathways inherent to the solvated molecule, J-aggregates also host nonradiative pathways that are idiosyncratic to their lattice. In order to design J-aggregates with unity QY, it is essential to overcome nonradiative pathways inherent to both the single chromophore and the J-aggregate. For example, it has been shown that nonradiative pathways in J-aggregates can be reduced by influencing their molecular packing and morphology using small molecules and surfactants.[18,20,27]

The fluorescence properties of Cy3UB J-aggregates reported here inspire the use of J-aggregates as high-speed light sources in emerging applications such as quantum computing, high color-purity displays and ultrafast optical communications.[14,29,58] In particular, ultrafast free-space optical-communication has the potential to transform the wireless infrastructure and enable more widespread and equitable internet access. Currently, a significant fraction of the world's population does not have access to the internet despite its vital role in accessing education, health-related information, and the broader job market. Free-space optical communication technologies are being explored to address this issue and provide internet services to underserved regions, where building wireless infrastructure is not financially viable.[59] Optical carriers enable multiple orders of magnitude higher speeds compared to the radio-frequencies used commonly in modern telecommunications. However, optical carriers must be efficiently captured and directed onto a fast photodetector for read-out. Recently, Facebook demonstrated an omnidirectional luminescent detector, which efficiently captured

and directed the incoming light onto a fast silicon APD, increasing the active area of the photodetector by more than an order of magnitude.[60] Using orthogonal frequency-division multiplexing, they achieved 2 Gbps data transfer rate, which was limited by the long 1.8 ns lifetime of the organic fluorophore. This work demonstrated the potential of luminescent detectors in high-speed optical communications while emphasizing the need for high-speed fluorescent materials.

Temperature-Dependent Spectroscopy of the Cy3UB J-Aggregates. J-type excitonic coupling is essential to develop highly emissive, short fluorescence lifetime materials in condensed phases. 2D molecular aggregates can host H-, I-, and J-type excitonic coupling between their constituent molecules.[22,44,45,50] In both H- and I-type excitonic coupling, fluorescence is almost completely quenched, whereas J-type excitonic coupling leads to a radiative rate enhancement and an increased QY.[29] Therefore, it is necessary to tune the structures of the monomers to favor the formation of highly emissive J-aggregates over I- or H-aggregates. While identifying H-aggregates is straightforward using steady-state absorption spectroscopy, I- and J-aggregates both have red-shifted spectra, making them difficult to distinguish. To further study excitonic coupling and superradiance in Cy3UB aggregates, we performed temperature-dependent absorption and emission spectroscopy, which can aid in distinguishing between I- and J-aggregates. We first stabilized the Cy3UB aggregates in a glassy sugar matrix consisting of 50% sucrose and 50% trehalose by weight. At room temperature, the absorption spectrum of Cy3UB aggregates in the sugar matrix is centered at 16,667 cm^{-1} (600 nm) with a full-width-at-half-maximum (FWHM) of 375 cm^{-1} (13.5 nm). As the temperature is reduced, the absorption spectrum blue-shifts, narrows and becomes more intense as shown in Fig.5A-C. At 79K, the absorption spectrum is centered at 16,795 cm^{-1} (595.4 nm) with a FWHM of 328 cm^{-1} (11.6 nm). The fluorescence spectrum of the Cy3UB

aggregates shows a similar behavior (Fig. 5D-F). At room-temperature, the fluorescence spectrum spectrum of Cy3UB aggregates in the sugar matrix is centered at 16,611 cm^{-1} (602 nm) with a FWHM of 275 cm^{-1}. As the temperature is decreased, the fluorescence spectrum shifts to lower wavelengths, narrows, and becomes more intense. At 79K, we observed strong fluorescence centered at 16756 cm^{-1} (596.8 nm) with a FWHM of 128 cm^{-1} (4.6 nm).

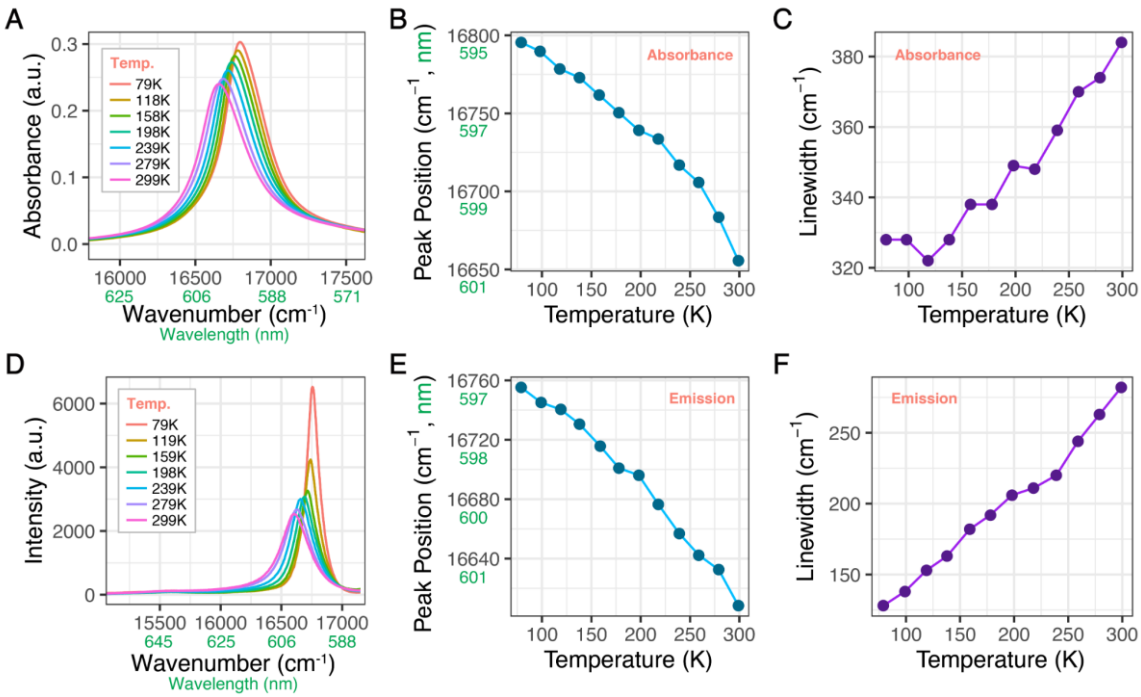

Figure 5. Temperature-Dependent Absorption Spectra of Cy3UB J-Aggregates. (**A**) Absorption spectra of J-aggregates at different temperatures. (**B**) Absorption peaks of J-aggregates at different temperatures. (**C**) Absorption FWHM at different temperatures. (**D**) Fluorescence spectra of J-aggregates at different temperatures. (**E**) Fluorescence peaks of J-aggregates at different temperatures. (**F**) Fluorescence FWHM at different temperatures.

This type of absorption and emission behavior suggests J-type excitonic coupling, which results in temperature dependent linewidths.[22,50] There are homogenous and inhomogenous contributions to the linewidth, where the former contribution arises due to the exciton's interaction with the environment at timescales faster than the lifetime of the exciton.

The inhomogeneous linewidth arises due to static energetic fluctuations across different molecular sites in the aggregate lattice and is temperature independent. The homogenous contribution can be expressed as the sum of (1) stimulated absorption/emission of phonons and (2) spontaneous emission of phonons and relaxation to the band edge.[22] The stimulated absorption/emission of phonons depends on the thermal occupation of phonons, and therefore, it is temperature dependent. In contrast, the spontaneous emission of phonons and relaxation to the band edge depends on the available density of states below the band edge, and is temperature independent. In J-aggregates, the lowest lying state is the optically bright state, and the linewidth shows strong temperature dependence due to the contribution (1). On the other hand, lower lying dark states below the I-band in I-aggregates can lead to the dominance of the contribution (2), which is temperature independent. Our temperature-dependent measurements support the formation of J-type excitonic coupling in Cy3UB aggregates. We speculate that the presence of four peripheral halogen atoms hinders the stacking of Cy3UB molecules, inducing a substantial shift between adjacent dyes in the aggregate lattice and leading to J-type excitonic coupling. This is consistent with the findings of Deshmukh et al., which shows that the nature of excitonic coupling in 2D molecular aggregates can be controlled by steric substituents.[22]

CONCLUSION

In conclusion, we have presented a novel bottom-up approach to develop highly emissive 2D molecular J-aggregates. We synthesized a J-aggregating cyanine dye with a conformationally restrained polymethine backbone. Due to the restriction of nonradiative C-C rotations within the polymethine backbone, the rigidized dye Cy3UB exhibits improved QY and longer lifetime compared to its unrigidized counterparts. Self-assembly of Cy3UB in a water-methanol mixture leads to extended J-aggregates with 2D sheet-like structures spanning

several microns in both dimensions. These J-aggregates have a strong absorption at 600 nm, a 50% quantum yield, and a 220 ps lifetime at room temperature. Temperature-dependent absorption and fluorescence spectroscopy confirms J-type excitonic coupling between the constituent molecules in the J-aggregate. These results support our hypothesis that reducing nonradiative processes in the monomer leads to J-aggregates with higher quantum yields. Moreover, comparison of the QY of the monomer and the J-aggregate highlights fundamental properties of nonradiative pathways in J-aggregates. In addition to nonradiative channels inherent to the solvated molecule, J-aggregates host new nonradiative pathways that are idiosyncratic to their lattice.

Our J-aggregates can be used as a model system to study exciton decay channels in molecular aggregates and potential ways to mitigate nonradiative losses. In addition, J-aggregates of Cy3UB can fill the need for high-speed light sources for information transmission applications. Finally, our approach can be utilized to develop the next generation of highly emissive J-aggregates with strong absorption cross sections, high QY, and short lifetimes. An immediate research avenue could be the exploration of J-aggregates of rigidized analogs of other commonly studied J-aggregating cyanine dyes. We believe that the method described here may produce new types of J-aggregates with unique optoelectronic properties.

ASSOCIATED CONTENT

Supporting Information. The supporting information is available free of charge on the ACS Publications website.

Synthesis and Characterization of Cy3UB, Dynamic Light Scattering, QY measurement, Calculation of Exciton Coherence Length (PDF)

AUTHOR INFORMATION

Corresponding Author

* E-mail: mgb@mit.edu. Phone: 617-497-0458

ORCID

Ulugbek Barotov: 0000-0002-8931-9127

Megan D. Klein: 0000-0002-0758-4294

Lili Wang: 0000-0002-6298-0302

Moungi G. Bawendi: 0000-0003-2220-4365

Notes

The authors declare no competing financial interest.

ACKNOWLEDGEMENTS

U.B. (lead author, project development, synthesis, data collection and analysis) was initially supported by the Institute for Soldier Nanotechnologies (award No. W911NF-13-D-0001) and then the National Science Foundation (award No. CHE-2108357). M.D.K. (J-aggregate lifetime measurement) was supported by a National Science Foundation Graduate Research Fellowship under Grant No. 1122374, as well as a grant from the Institute for Soldier Nanotechnologies (award No. W911NF-18-2-0048). L.W. (lifetime measurement) was supported by the Department of Energy, Office of Basic Energy Sciences, Division of Material Sciences and Engineering (award No. DE-SC0021650). Specimens were prepared and imaged at the Cryogenic Electron Microscopy Facility in MIT.nano on the Talos Arctica, which was a gift from the Arnold and Mabel Beckman Foundation. We thank Edward J. Brignole in the MIT.nano Cryo-EM Facility for his guidance on cryo-TEM sample preparation and imaging.

We would like to also thank Arundhati P. Deshmukh for fruitful discussions regarding the cryo-sample preparation and imaging of 2D molecular aggregates.

Present Addresses

‡Department of Chemistry, University of Washington, Seattle, Washington 98195, USA

REFERENCES

(1) Lakowicz, J. R. *Principles of Fluorescence Spectroscopy*; Springer Science & Business Media, 2013.

(2) García de Arquer, F. P.; Talapin, D. V.; Klimov, V. I.; Arakawa, Y.; Bayer, M.; Sargent, E. H. Semiconductor Quantum Dots: Technological Progress and Future Challenges. *Science* **2021**, *373* (6555).

(3) Feng, G.; Kwok, R. T. K.; Tang, B. Z.; Liu, B. Functionality and Versatility of Aggregation-Induced Emission Luminogens. *Applied Physics Reviews*. **2017**, *4* (021307).

(4) Mei, J.; Leung, N. L. C.; Kwok, R. T. K.; Lam, J. W. Y.; Tang, B. Z. Aggregation-Induced Emission: Together We Shine, United We Soar! *Chemical Reviews*. **2015**, *115*, 21, 11718–11940.

(5) Bruns, O. T.; Bischof, T. S.; Harris, D. K.; Franke, D.; Shi, Y.; Riedemann, L.; Bartelt, A.; Jaworski, F. B.; Carr, J. A.; Rowlands, C. J.; Wilson, M. W. B.; Chen, O.; Wei, H.; Hwang, G. W.; Montana, D. M.; Coropceanu, I.; Achorn, O. B.; Kloepper, J.; Heeren, J.; So, P. T. C.; Fukumura, D.; Jensen, K. F.; Jain, R. K.; Bawendi, M. G. Next-Generation Optical Imaging with Short-Wave Infrared Quantum Dots. *Nat Biomed Eng* **2017**, *1*

(6) van Amerongen, H.; van Grondelle, R.; Valkunas, L. Photosynthetic Excitons. **2000**.

(7) Purcell, E. M.; Torrey, H. C.; Pound, R. V. Resonance Absorption by Nuclear Magnetic Moments in a Solid. *Physical Review*. **1946**, *69*, 37–38.

(8) Tam, F.; Goodrich, G. P.; Johnson, B. R.; Halas, N. J. Plasmonic Enhancement of Molecular Fluorescence. *Nano Letters*. **2007**, *7*, 2, 496–501.

(9) Hoang, T. B.; Akselrod, G. M.; Argyropoulos, C.; Huang, J.; Smith, D. R.; Mikkelsen, M. H. Ultrafast Spontaneous Emission Source Using Plasmonic Nanoantennas. *Nat. Commun.* **2015**, *6*, 7788.

(10) Boriskina, S. V.; Cooper, T. A.; Zeng, L.; Ni, G.; Tong, J. K.; Tsurimaki, Y.; Huang, Y.; Meroueh, L.; Mahan, G.; Chen, G. Losses in Plasmonics: From Mitigating Energy Dissipation to Embracing Loss-Enabled Functionalities. *Advances in Optics and Photonics*. **2017**, *9,* 775-827.

(11) Skribanowitz, N.; Herman, I. P.; MacGillivray, J. C.; Feld, M. S. Observation of Dicke Superradiance in Optically Pumped HF Gas. *Physical Review Letters*. **1973**, *30,* 309–312.

(12) Scheibner, M.; Schmidt, T.; Worschech, L.; Forchel, A.; Bacher, G.; Passow, T.; Hommel, D. Superradiance of Quantum Dots. *Nature Physics*. **2007**, *3,* 106–110.

(13) Spano, F. C.; Mukamel, S. Superradiance in Molecular Aggregates. *The Journal of Chemical Physics*. **1989**, *91,* 683–700.

(14) Zhao, H.; Zhao, Y.; Song, Y.; Zhou, M.; Lv, W.; Tao, L.; Feng, Y.; Song, B.; Ma, Y.; Zhang, J.; Xiao, J.; Wang, Y.; Lien, D.-H.; Amani, M.; Kim, H.; Chen, X.; Wu, Z.; Ni, Z.; Wang, P.; Shi, Y.; Ma, H.; Zhang, X.; Xu, J.-B.; Troisi, A.; Javey, A.; Wang, X. Strong Optical Response and Light Emission from a Monolayer Molecular Crystal. *Nat. Commun.* **2019**, *10* (1), 5589.

(15) Sharma, A.; Zhang, L.; Tollerud, J. O.; Dong, M.; Zhu, Y.; Halbich, R.; Vogl, T.; Liang, K.; Nguyen, H. T.; Wang, F.; Sanwlani, S.; Earl, S. K.; Macdonald, D.; Lam, P. K.; Davis, J. A.; Lu, Y. Supertransport of Excitons in Atomically Thin Organic Semiconductors at the 2D Quantum Limit. *Light: Science & Applications*. **2020**, *9 (116).*

(16) Caram, J. R.; Doria, S.; Eisele, D. M.; Freyria, F. S.; Sinclair, T. S.; Rebentrost, P.; Lloyd,

S.; Bawendi, M. G. Room-Temperature Micron-Scale Exciton Migration in a Stabilized Emissive Molecular Aggregate. *Nano Lett.* **2016**, *16* (11), 6808–6815.

(17) Doria, S.; Sinclair, T. S.; Klein, N. D.; Bennett, D. I. G.; Chuang, C.; Freyria, F. S.; Steiner, C. P.; Foggi, P.; Nelson, K. A.; Cao, J.; Aspuru-Guzik, A.; Lloyd, S.; Caram, J. R.; Bawendi, M. G. Photochemical Control of Exciton Superradiance in Light-Harvesting Nanotubes. *ACS Nano* **2018**, *12* (5), 4556–4564.

(18) De Rossi, U.; Daehne, S.; Lindrum, M. Increased Coupling Size in J-Aggregates throughN-N-Alkyl Betaine Surfactants. *Langmuir* **1996**, *12* (5), 1159–1165.

(19) Obara, Y.; Saitoh, K.; Oda, M.; Tani, T. Room-Temperature Fluorescence Lifetime of Pseudoisocyanine (PIC) J Excitons with Various Aggregate Morphologies in Relation to Microcavity Polariton Formation. *Int. J. Mol. Sci.* **2012**, *13* (5), 5851–5865.

(20) Guralchuk, G. Y.; Katrunov, I. K.; Grynyov, R. S.; Sorokin, A. V.; Yefimova, S. L.; Borovoy, I. A.; Malyukin, Y. V. Anomalous Surfactant-Induced Enhancement of Luminescence Quantum Yield of Cyanine Dye J-Aggregates. *The Journal of Physical Chemistry C*. **2008**, *112,* 38, 14762–14768.

(21) Shao, C.; Xiao, F.; Guo, H.; Yu, J.; Jin, D.; Wu, C.; Xi, L.; Tian, L. Utilizing Polymer Micelle to Control Dye J-Aggregation and Enhance Its Theranostic Capability. *iScience* **2019**, *22*, 229–239.

(22) Deshmukh, A.; Koppel, D.; Chuang, C.; Cadena, D.; Cao, J.; Caram, J. Design Principles for 2-Dimensional Molecular Aggregates Using Kasha's Model: Tunable Photophysics in Near and Shortwave Infrared. *The Journal of Physical Chemistry C **2019**, 123,* 30, 18702-18710.

(23) Moll, J.; Daehne, S.; Durrant, J. R.; Wiersma, D. A. Optical Dynamics of Excitons in J Aggregates of a Carbocyanine Dye. *The Journal of Chemical Physics*. **1995**, 102, 6362–6370.

(24) Malyukin, Y. V.; Sorokin, A. V.; Semynozhenko, V. P. Features of Exciton Dynamics in Molecular Nanoclusters (J-Aggregates): Exciton Self-Trapping (Review Article). *Low Temperature Physics*. **2016**, *42,* 429–440.

(25) Spano, F. C. The Spectral Signatures of Frenkel Polarons in H- and J-Aggregates. *Acc. Chem. Res.* **2010**, *43* (3), 429–439.

(26) Evidence of Exciton Self-Trapping in Pseudoisocyanine J-Aggregates Formed in Layered Polymer Films. *J. Phys. Chem. C* **2015**, 119, 49, 27865-27873.

(27) Anantharaman, S. B.; Kohlbrecher, J.; Rainò, G.; Yakunin, S.; Stöferle, T.; Patel, J.; Kovalenko, M.; Mahrt, R. F.; Nüesch, F. A.; Heier, J. Enhanced Room-Temperature Photoluminescence Quantum Yield in Morphology Controlled J-Aggregates. *Adv. Sci.* **2021**, *8* (4), 1903080.

(28) Ishchenko, A. A. Structure and Spectral-Luminescent Properties of Polymethine Dyes. *Russ. Chem. Rev.* **1991**, *60* (8), 865.

(29) Bricks, J. L.; Slominskii, Y. L.; Panas, I. D.; Demchenko, A. P. Fluorescent J-Aggregates of Cyanine Dyes: Basic Research and Applications Review. *Methods Appl Fluoresc* **2017**, *6* (1), 012001.

(30) Kolesnikov, A. M.; Mikhailenko, F. A. The Conformations of Polymethine Dyes. *Russ. Chem. Rev.* **1987**, *56* (3), 275–287.

(31) Hart, S. M.; Banal, J. L.; Bathe, M.; Schlau-Cohen, G. S. Identification of Nonradiative Decay Pathways in Cy3. *J. Phys. Chem. Lett.* **2020**, *11* (13), 5000–5007.

(32) Cooper, M.; Ebner, A.; Briggs, M.; Burrows, M.; Gardner, N.; Richardson, R.; West, R. Cy3B: Improving the Performance of Cyanine Dyes. *J. Fluoresc.* **2004**, *14* (2), 145–150.

(33) Michie, M. S.; Götz, R.; Franke, C.; Bowler, M.; Kumari, N.; Magidson, V.; Levitus, M.; Loncarek, J.; Sauer, M.; Schnermann, M. J. Cyanine Conformational Restraint in the Far-Red Range. *J. Am. Chem. Soc.* **2017**, *139* (36), 12406–12409.

(34) Kobayashi, T. *J-Aggregates*. World Scientific, **1996**.

(35) Würthner, F.; Kaiser, T. E.; Saha-Möller, C. R. J-Aggregates: From Serendipitous Discovery to Supramolecular Engineering of Functional Dye Materials. *Angew. Chem. Int. Ed Engl.* **2011**, *50* (15), 3376–3410.

(36) Tani, T. *Photographic Sensitivity: Theory and Mechanisms*; Oxford University Press on Demand, 1995.

(37) Lincoln, L. L.; Heseltine, D. W. 7aH,8aH-bisbenzothiazolo(3,2-a;-3',2'-a)pyrano [3,2-c;5,6-c]Dipyridinium Compounds and Related Derivatives Thereof. 3904637, September 9, 1975.

(38) Fennel, F.; Gershberg, J.; Stolte, M.; Würthner, F. Fluorescence Quantum Yields of Dye Aggregates: A Showcase Example Based on Self-Assembled Perylene Bisimide Dimers. *Phys. Chem. Chem. Phys.* **2018**, *20* (11), 7612–7620.

(39) Würth, C.; Grabolle, M.; Pauli, J.; Spieles, M.; Resch-Genger, U. Comparison of Methods and Achievable Uncertainties for the Relative and Absolute Measurement of Photoluminescence Quantum Yields. *Anal. Chem.* **2011**, *83* (9), 3431–3439.

(40) Pawlik, A.; Ouart, A.; Kirstein, S.; Abraham, H.-W.; Daehne, S. Synthesis and UV/Vis Spectra of J-Aggregating 5,5′,6,6′-Tetrachlorobenzimidacarbocyanine Dyes for Artificial Light-Harvesting Systems and for Asymmetrical Generation of Supramolecular Helices. *European J. Org. Chem.* **2003**, *2003* (16), 3065–3080.

(41) Kriete, B.; Bondarenko, A. S.; Jumde, V. R.; Franken, L. E.; Minnaard, A. J.; Jansen, T. L. C.; Knoester, J.; Pshenichnikov, M. S. Steering Self-Assembly of Amphiphilic Molecular Nanostructures via Halogen Exchange. *J. Phys. Chem. Lett.* **2017**, *8* (13), 2895–2901.

(42) Hall, L. M.; Gerowska, M.; Brown, T. A Highly Fluorescent DNA Toolkit: Synthesis and Properties of Oligonucleotides Containing New Cy3, Cy5 and Cy3B Monomers. *Nucleic*

Acids Res. **2012**, *40* (14), e108.

(43) Weigend, F.; Ahlrichs, R. Balanced Basis Sets of Split Valence, Triple Zeta Valence and Quadruple Zeta Valence Quality for H to Rn: Design and Assessment of Accuracy. *Phys. Chem. Chem. Phys.* **2005**, *7* (18), 3297–3305.

(44) Kasha, M. Energy Transfer Mechanisms and The Molecular Exciton Model for Molecular Aggregates. *Radiat. Res.* **1963**, *20*, 55–70.

(45) Zheng, C.; Zhong, C.; Collison, C. J.; Spano, F. C. Non-Kasha Behavior in Quadrupolar Dye Aggregates: The Red-Shifted H-Aggregate. *The Journal of Physical Chemistry C* **2019**, *123,* 5, 3203–3215.

(46) von Berlepsch, H.; Kirstein, S.; Hania, R.; Pugzlys, A.; Böttcher, C. Modification of the Nanoscale Structure of the J-Aggregate of a Sulfonate-Substituted Amphiphilic Carbocyanine Dye through Incorporation of Surface-Active Additives. *J. Phys. Chem. B* **2007**, *111* (7), 1701–1711.

(47) Eisele, D. M.; Cone, C. W.; Bloemsma, E. A.; Vlaming, S. M.; van der Kwaak, C. G. F.; Silbey, R. J.; Bawendi, M. G.; Knoester, J.; Rabe, J. P.; Vanden Bout, D. A. Utilizing Redox-Chemistry to Elucidate the Nature of Exciton Transitions in Supramolecular Dye Nanotubes. *Nat. Chem.* **2012**, *4* (8), 655–662.

(48) Eisele, D. M.; Arias, D. H.; Fu, X.; Bloemsma, E. A.; Steiner, C. P.; Jensen, R. A.; Rebentrost, P.; Eisele, H.; Tokmakoff, A.; Lloyd, S.; Nelson, K. A.; Nicastro, D.; Knoester, J.; Bawendi, M. G. Robust Excitons Inhabit Soft Supramolecular Nanotubes. *Proc. Natl. Acad. Sci*. **2014**, *111* (33), E3367–E3375.

(49) Kasha, M.; Rawls, H. R.; Ashraf El-Bayoumi, M. The Exciton Model in Molecular Spectroscopy. *Pure and Applied Chemistry*. **1965**, *11* (3-4)*,* 371–392.

(50) Chuang, C.; Bennett, D. I. G.; Caram, J. R.; Aspuru-Guzik, A.; Bawendi, M. G.; Cao, J. Generalized Kasha's Model: T-Dependent Spectroscopy Reveals Short-Range Structures

of 2D Excitonic Systems. *Chem*. **2019**, *5,* 12, 3135–3150.

(51) Jelley, E. E. Spectral Absorption and Fluorescence of Dyes in the Molecular State. *Nature*. **1936**, *138,* 1009–1010.

(52) Bricker, W. P.; Banal, J. L.; Stone, M. B.; Bathe, M. Molecular Model of J-Aggregated Pseudoisocyanine Fibers. *J. Chem. Phys.* **2018**, *149* (2), 024905.

(53) Berlepsch, H. von; von Berlepsch, H.; Böttcher, C.; Dähne, L. Structure of J-Aggregates of Pseudoisocyanine Dye in Aqueous Solution. *J. Phys. Chem. B **2000,** 104,* 37, 8792–8799.

(54) Deshmukh, A. P.; Bailey, A. D.; Forte, L. S.; Shen, X.; Geue, N.; Sletten, E. M.; Caram, J. R. Thermodynamic Control over Molecular Aggregate Assembly Enables Tunable Excitonic Properties across the Visible and Near-Infrared. *J. Phys. Chem. Lett.* **2020**, *11,* 19, 8026–8033.

(55) Knapp, E. W. Lineshapes of Molecular Aggregates, Exchange Narrowing and Intersite Correlation. *Chemical Physics*. **1984**, *85,* 1, 73–82.

(56) Brixner, T.; Hildner, R.; Köhler, J.; Lambert, C.; Würthner, F. Exciton Transport in Molecular Aggregates - From Natural Antennas to Synthetic Chromophore Systems. *Adv. Energy Mater.* **2017**, *7,* 1700236.

(57) Lebedenko, A. N.; Grynyov, R. S.; Guralchuk, G. Y.; Sorokin, A. V.; Yefimova, S. L.; Malyukin, Y. V. Coherent Mechanism of Exciton Transport in Disordered J-Aggregates. *J. Phys. Chem. C* **2009**, *113,* 29, 12883–12887.

(58) Zhao, Y.; Wang, V.; Javey, A. Molecular Materials with Short Radiative Lifetime for High-Speed Light-Emitting Devices. *Matter*. **2020**, *3,* 6, 1832–1844.

(59) Bouchet, O.; Sizun, H.; Boisrobert, C.; de Fornel, F. *Free-Space Optics: Propagation and Communication*; John Wiley & Sons, 2010.

(60) Peyronel, T.; Quirk, K. J.; Wang, S. C.; Tiecke, T. G. Luminescent Detector for Free-

Space Optical Communication. *Optica* **2016**, *3* (7), 787.

TOC Graphic: